Electronic Companion – A Novel Framework for the Day-Ahead Market Clearing Process Featuring the Participation of Distribution System Operators and a Hybrid Pricing Mechanism

Wandry R. Faria, Gregorio Muñoz-Delgado, *Senior Member IEEE*, Javier Contreras, *Fellow IEEE*, and Benvindo R. Pereira Jr.

NOMENCLATURE

In this section, additional variables related to the lower-level dual problem are defined.

$\overline{\alpha}_{g,t,s}$, $\underline{\alpha}_{g,t,s}$ Dual variables associated with the upper and lower bounds for the power injection of distribution-connected generators.

$\overline{\beta}_{i,t,s}$, $\underline{\beta}_{i,t,s}$ Dual variables associated with the upper and lower bounds for the load shift.

$\gamma_{i,s}$ Dual variable associated with the zero-sum of load shifting over the planning horizon.

$\epsilon_{i,s}$ Dual variable associated with the storage system's energy conservation considering the initial and final periods.

$\overline{\theta}_{i,t,s}$, $\underline{\theta}_{i,t,s}$ Dual variables associated with the upper and lower bounds for the power injection of transmission-connected generators.

$\overline{\omega}_{ij,t,s}$, $\underline{\omega}_{ij,t,s}$ Dual variables associated with the upper and lower bounds for the power flow across distribution lines.

$\overline{\kappa}_{i,t,s}$, $\underline{\kappa}_{i,t,s}$ Dual variables associated with the upper and lower bounds for the substations' capacities.

$\lambda_{i,t,s}$ Dual variable associated with the power balance at distribution nodes.

$\mu_{ij,t,s}$ Dual variable associated with the distribution system voltage drop calculation.

$\overline{\sigma}_{i,t,s}$, $\underline{\sigma}_{i,t,s}$ Dual variables associated with the upper and lower bounds for the storage systems' charge/discharge.

$\overline{\phi}_{i,t,s}$, $\underline{\phi}_{i,t,s}$ Dual variables associated with the upper and lower bounds for the state of charge of the storage systems.

$\overline{\varphi}_{i,t,s}$, $\underline{\varphi}_{i,t,s}$ Dual variables associated with the upper and lower bounds for the voltage of distribution nodes.

$\Omega_{i,t,s}$ Dual variable associated with the calculation of the energy storage systems' state of charge.

I. REFORMULATION AS A MPEC

As a general rule, adopting the strong duality theorem to formulate the mathematical programming with equilibrium constraints (MPEC) model leads to lower computational burden than using Karush–Kuhn–Tucker (KKT) conditions, as shown in [EC.1]. However, for this specific problem, the linearization of the bilinear terms in the leader's objective function has an even heavier computational effort than the KKT conditions if the primal-dual model is employed to describe the MPEC model, as observed in [EC.2],[EC.3]. Thus, the MPEC model is formulated using KKT conditions as follows.

$$\min\sum_{s\in S}\xi_s\sum_{t\in T}\left[\sum_{g\in G_T}\left(\pi_{g,t,s}P^T_{g,t,s}\right)-\sum_{i\in N_\infty}\left(\pi_{i,t,s}P^{SE}_{i,t,s}\right)\right] \tag{EC.1}$$

subject to:

Constraints (2)–(7): Upper-level constraints

Constraint (9): GENCO's primal constraints

Constraints (11)–(24): DSO's primal constraints

$$\xi_s\left(2a_gP^T_{g,t,s}+b_g-\pi_{g,t,s}\right)+\overline{\theta}_{g,t,s}-\underline{\theta}_{g,t,s}=0 \quad \forall g\in G_T,t\in T,s\in S \tag{EC.2}$$

$$\xi_s\left(2a_gP^D_{g,t,s}+b_g\right)-\lambda_{i,t,s}+\overline{\alpha}_{g,t,s}+\underline{\alpha}_{g,t,s}=0 \quad \forall g\in G_D,t\in T,s\in S \tag{EC.3}$$

$$\lambda_{i,t,s}-\lambda_{j,t,s}+Z_{ij}\mu_{ij,t,s}+\overline{\omega}_{ij,t,s}-\underline{\omega}_{ij,t,s}=0 \quad \forall ij\in L_D,t\in T,s\in S \tag{EC.4}$$

$$\xi_s\pi_{i,t,s}-\lambda_{i,t,s}+\overline{\kappa}_{i,t,s}-\underline{\kappa}_{i,t,s}=0 \quad \forall i\in N_\infty,t\in T,s\in S \tag{EC.5}$$

$$\lambda_{i,t,s}+\overline{\beta}_{i,t,s}-\underline{\beta}_{i,t,s}-\gamma_i=0 \quad \forall i\in N_D,t\in T,s\in S \tag{EC.6}$$

$$-\lambda_{i,t,s}+\overline{\sigma}_{i,t,s}-\underline{\sigma}_{i,t,s}+\Omega_{i,t,s}=0 \quad \forall i\in N_D,t\in T,s\in S \tag{EC.7}$$

$$\overline{\phi}_{i,t,s}-\underline{\phi}_{i,t,s}+\Omega_{i,t,s}-\Omega_{i,t+1,s}=0 \quad \forall i\in N_D,t<H,s\in S \tag{EC.8}$$

$$\overline{\phi}_{i,H,s}-\underline{\phi}_{i,H,s}+\Omega_{i,H,s}-\epsilon_{i,s}=0 \quad \forall i\in N_D,s\in S \tag{EC.9}$$

$$-\sum_{ij\in L_D}\omega_{ij,t,s}+\sum_{ki\in L_D}\omega_{ki,t,s}+\overline{\varphi}_{i,t,s}-\underline{\varphi}_{i,t,s}=0 \quad \forall i\in N_D,t\in T,s\in S \tag{EC.10}$$

$$\overline{\theta}_{g,t,s}(-P^T_{g,t,s}+\overline{P}^T_g)=0 \quad \forall g\in G_T,t\in T,s\in S \tag{EC.11}$$

$$\underline{\theta}_{g,t,s}(P^T_{g,t,s}-\underline{P}^T_g)=0 \quad \forall g\in G_T,t\in T,s\in S \tag{EC.12}$$

$$\overline{\omega}_{ij,t,s}(-P_{ij,t,s}+\overline{P}_{ij})=0 \quad \forall ij\in L_D,t\in T,s\in S \tag{EC.13}$$

$$\underline{\omega}_{ij,t,s}(P_{ij,t,s}+\overline{P}_{ij})=0 \quad \forall ij\in L_D,t\in T,s\in S \tag{EC.14}$$

$$\overline{\varphi}_{i,t,s}(-V_{i,t,s}+\overline{V}_i)=0 \quad \forall i\in N_D,t\in T,s\in S \tag{EC.15}$$

$$\underline{\varphi}_{i,t,s}(V_{i,t,s}-\underline{V}_i)=0 \quad \forall i\in N_D,t\in T,s\in S \tag{EC.16}$$

$$\overline{\alpha}_{g,t,s}(-P^D_{g,t,s}+\overline{P}^D_g)=0 \quad \forall g\in G_D,t\in T,s\in S \tag{EC.17}$$

$$\underline{\alpha}_{g,t,s}(P^D_{g,t,s}-\underline{P}^D_g)=0 \quad \forall g\in G_D,t\in T,s\in S \tag{EC.18}$$

$$\overline{\kappa}_{ij,t,s}(-P^{SE}_{i,t,s}+\overline{P}^{SE})=0 \quad \forall i\in N_\infty,t\in T,s\in S \tag{EC.19}$$

$$\underline{\kappa}_{ij,t,s}(P^{SE}_{i,t,s}+\overline{P}^{SE})=0 \quad \forall i\in N_\infty,t\in T,s\in S \tag{EC.20}$$

$$\overline{\beta}_{i,t,s}(-P^{LS}_{i,t,s}+\overline{P}^{LS}_{i})=0 \quad \forall i\in N_D,t\in T,s\in S \tag{EC.21}$$

$$\underline{\beta}_{i,t,s}(P^{LS}_{i,t,s}-\underline{P}^{LS}_{i})=0 \quad \forall i\in N_D,t\in T,s\in S \tag{EC.22}$$

$$\overline{\sigma}_{i,t,s}(-P^{ESS}_{i,t,s}+\overline{P}^{ESS}_{i})=0 \quad \forall i\in N_D,t\in T,s\in S \tag{EC.23}$$

$$\underline{\sigma}_{i,t,s}(P^{ESS}_{i,t,s}-\underline{P}^{ESS}_{i})=0 \quad \forall i\in N_D,t\in T,s\in S \tag{EC.24}$$

$$\overline{\phi}_{i,t,s}(-SOC_{i,t,s}+\overline{SOC}_{i})=0 \quad \forall i\in N_D,t\in T,s\in S \tag{EC.25}$$

$$\underline{\phi}_{i,t,s}(SOC_{i,t,s}-\underline{SOC}_{i})=0 \quad \forall i\in N_D,t\in T,s\in S \tag{EC.26}$$

$$\overline{\theta}_{g,t,s}\geq 0 \qquad \underline{\theta}_{g,t,s}\geq 0 \quad \forall g\in G_T,t\in T,s\in S \tag{EC.27}$$

$$\overline{\alpha}_{g,t,s}\geq 0 \qquad \underline{\alpha}_{g,t,s}\geq 0 \quad \forall g\in G_D,t\in T,s\in S \tag{EC.28}$$

$$\overline{\kappa}_{i,t,s}\geq 0 \qquad \underline{\kappa}_{i,t,s}\geq 0 \quad \forall i\in N_\infty,t\in T,s\in S \tag{EC.29}$$

$$\overline{\omega}_{ij,t,s}\geq 0 \qquad \underline{\omega}_{ij,t,s}\geq 0 \quad \forall ij\in L_D,t\in T,s\in S \tag{EC.30}$$

$$\overline{\varphi}_{i,t,s}\geq 0 \qquad \underline{\varphi}_{i,t,s}\geq 0 \quad \forall i\in N_D,t\in T,s\in S \tag{EC.31}$$

$$\overline{\beta}_{i,t,s}\geq 0 \qquad \underline{\beta}_{i,t,s}\geq 0 \quad \forall i\in N_D,t\in T,s\in S \tag{EC.32}$$

$$\overline{\sigma}_{i,t,s}\geq 0 \qquad \underline{\sigma}_{i,t,s}\geq 0 \quad \forall i\in N_D,t\in T,s\in S \tag{EC.33}$$

$$\overline{\phi}_{i,t,s}\geq 0 \qquad \underline{\phi}_{i,t,s}\geq 0 \quad \forall i\in N_D,t\in T,s\in S \tag{EC.34}$$

Equations (EC.2)–(EC.10) are the KKT stationary conditions, while equations (EC.11)–(EC.26) represents the complementary slackness conditions. Finally (EC.27)–(EC.34) are the dual feasibility constraints.

Observe in (EC.2) that the energy price is equal to the derivative of the cost function applied at the power injection value, i.e., $\pi_{g,t,s} = 2a_g P^T_{g,t,s} + b_g$ whenever $0 < P^T_{g,t,s} < \overline{P}^T_g$, since $\overline{\theta}_{g,t,s}$ and $\underline{\theta}_{g,t,s}$ can be different of zero only when the generator is operating at upper or lower bound, respectively. Note that, if $P^T_{g,t,s}=0$ then $\underline{\theta}_{g,t,s}\geq 0$ and $\pi_{g,t,s}\leq 2a_g P^T_{g,t,s}+b_g$. Analogously, $\pi_{g,t,s} \geq 2a_g P^T_{g,t,s} + b_g$ if $P^T_{g,t,s} = \overline{P}^T_g$. Thus, whenever there is power injection, the hourly nodal price $\pi_{g,t,s}$ has to be at least equal to the derivative of the cost function applied at the power injection value. Given the convex formulation of the generation costs, the value given by the integral of the generation curve from zero to the power injection value, i.e., the total generation costs, will always be lower than that of the product between the nodal price $\pi_{g,t,s}$ and the power injection $P^T_{g,t,s}$ for $P^T_{g,t,s}>0$. Thus, profit is guaranteed whenever the generator injects power into the transmission system.

II. Mixed-Integer Problem Formulation

The nonlinear equations described in (EC.11)–(EC.26) can be linearized using the Big-M method. An example is presented for (EC.11), which is rewritten as (EC.35)–(EC.36). The same procedure is applied to the other complementary slackness equations.

$$\overline{\theta}_{g,t,s}\leq M z^{\overline{\theta}}_{g,t,s} \quad \forall g\in G_T,t\in T,s\in S \tag{EC.35}$$

$$(-P^T_{g,t,s}+\overline{P}^T_g)\leq M(1-z^{\overline{\theta}}_{g,t,s}) \quad \forall g\in G_T,t\in T,s\in S \tag{EC.36}$$

being $z^{\overline{\theta}}$ a binary variable that indicates that the constraint $P^T_{g,t,s}\leq \overline{P}^T_g$ is active, i.e., $P^T_{g,t,s}=\overline{P}^T_g$. M is a sufficiently large constant.

As for the linearization of the bilinear terms in (EC.1), namely $(\pi_{g,t,s}P^T_{g,t,s})$ and $(\pi_{dso,t,s}P^{SE}_{t,s})$, the following steps were taken.

A. Cost of Trading Power with GENCOs

From the strong duality theorem, we know that the primal and dual objective functions of the generation company (GENCO) model assume the same value at the optimal solution as follows.

$$\sum_{s\in S}\xi_s\sum_{t\in T}\sum_{g\in G_T}\left(a_g P^{T^2}_{g,t,s}+b_g P^T_{g,t,s}+c_g-\pi_{g,t,s}P^T_{g,t,s}\right)= \sum_{s\in S}\sum_{t\in T}\sum_{g\in G_T}\left(\overline{P}^T_g\overline{\theta}_{g,t,s}-\underline{P}^T_g\underline{\theta}_{g,t,s}\right) \tag{EC.37}$$

Hence, one can rewrite the bilinear term as follows.

$$\sum_{s\in S}\xi_s\sum_{t\in T}\sum_{g\in G_T}\pi_{g,t,s}P^T_{g,t,s}=\sum_{s\in S}\sum_{t\in T}\sum_{g\in G_T}\Big[-\overline{P}^T_g\overline{\theta}_{g,t,s} +\underline{P}^T_g\underline{\theta}_{g,t,s}+\xi_s\left(a_g P^{T^2}_{g,t,s}+b_g P^T_{g,t,s}+c_g\right)\Big] \tag{EC.38}$$

Finally, the quadratic function that describes the generation costs can be linearized via piecewise linearization. The linearized generation cost of generator g at period t and scenario s will be referred to as $GC_{g,t,s}$. Hence, the linear form of the bilinear term is given by:

$$\sum_{s\in S}\xi_s\sum_{t\in T}\sum_{g\in G_T}\left(\pi_{g,t,s}P^T_{g,t,s}\right)=\sum_{s\in S}\sum_{t\in T}\sum_{g\in G_T}\Big(\xi_s GC_{g,t,s} -\overline{P}^T_g\overline{\theta}_{g,t,s}+\underline{P}^T_g\underline{\theta}_{g,t,s}\Big) \tag{EC.39}$$

B. Cost/revenue of Trading Power with the DSO

Applying the strong duality theorem for the distribution system operator (DSO) model, one can write the following equation.

$$\begin{aligned}&\sum_{s\in S}\xi_s\sum_{t\in T}\Bigg[\sum_{g\in G_D}\left(a_g P^{D^2}_{g,t,s}+b_g P^D_{g,t,s}+c_g\right) +\sum_{i\in N_\infty}\left(\pi_{i,t,s}P^{SE}_{i,t,s}\right)\Bigg]=\sum_{s\in S}\sum_{t\in T}\Bigg[\sum_{n\in N_D}\Big(L_{i,t,s}\lambda_{i,t,s}\\ &-\overline{V}_n\overline{\varphi}_{i,t,s}+\underline{V}_n\underline{\varphi}_{i,t,s}-\overline{P}^{LS}_{i,t,s}\overline{\beta}_{i,t,s}+\underline{P}^{LS}_{i,t,s}\underline{\beta}_{i,t,s}\\ &-\overline{P}^{ESS}_{i,t,s}\overline{\sigma}_{i,t,s}+\underline{P}^{ESS}_{i,t,s}\underline{\sigma}_{i,t,s}-\overline{SOC}_{i,t,s}\overline{\phi}_{i,t,s}\\ &+\underline{SOC}_{i,t,s}\underline{\phi}_{i,t,s}\Big)-\sum_{ij\in L_D}\left(\overline{P}_{ij}(\overline{\omega}_{ij,t,s}+\underline{\omega}_{ij,t,s})\right)\\ &-\sum_{i\in N_\infty}\left(\overline{P}^{SE}_i(\overline{\kappa}_{i,t,s}+\underline{\kappa}_{i,t,s})\right)+\sum_{g\in G_D}\left(-\overline{\alpha}_{g,t,s}\overline{P}^D_g+\underline{\alpha}_{g,t,s}\underline{P}^D_g\right)\Bigg]\\ &+\sum_{s\in S}\sum_{n\in N_D}\left(SOC^0_{i,s}(\epsilon_{i,s}-\Omega_{i,1,s})\right)\end{aligned} \tag{EC.40}$$

Henceforth, the right-hand side of (EC.40) will be referred to as **B**. Observe that **B** is a linear function. Thus, $\pi_{i,t,s}P^{SE}_{i,t,s}$ can be written as:

$$\sum_{s\in S}\xi_s\sum_{t\in T}\sum_{i\in N_\infty}\left(\pi_{i,t,s}P^{SE}_{i,t,s}\right)=\mathbf{B}-\sum_{s\in S}\sum_{t\in T}\sum_{g\in G_D}\left(\xi_s GC_{g,t,s}\right) \tag{EC.41}$$

III. Illustrative Example for the Proposed Hybrid Pricing Method

Consider the simple three-node transmission system shown in Fig. EC.1. Assume that 1) all lines have the same reactance of 0.25 p.u., 2) losses can be ignored, 3) the demand is inelastic, and 4) the lines' capacities and the generators' power injection are unlimited. Thus, the system demand would be supplied entirely by G3 and the energy price on every node would be 5 \$/MWh (exactly the market clearing price (MCP) since there is no congestion). The result obtained for both the traditional and the proposed models are the same in this case. Since there are no line limits ($\overline{PF}=\infty$), (25) is rewritten as $w_{l,t,s} \leq (1-u)$. Thus, the binary variable w is always zero as long as $u > 0$. As a result, the binary variable $s=0$ for every node (see (27)) and sets the congestion price quota (CP) on every node as zero (see (28)). Hence, the energy prices are the same for the entire system. The system's shadow prices (local marginal price (LMP)) and the values found using the proposed pricing mechanism (π) are shown in Fig. EC.1.

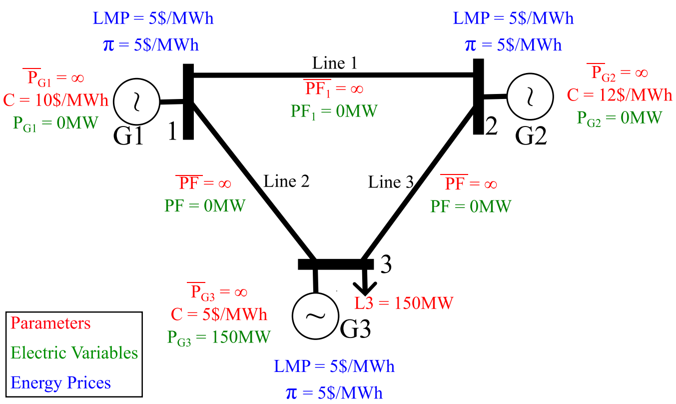

Fig. EC.1. Theoretical Example 1

Next, consider a system with the same topology but with the injection and power flow limits shown in Fig. EC.2. The resulting power flow and nodal prices are illustrated in Fig. EC.2. It can be observed that line 1 operates at its limit in this case. Since there is congestion, the LMPs are not the same for every node, as shown in the figure. According to the shadow prices, the energy price at nodes 1, 2 and 3 should be, respectively, 10 \$/MWh, 12 \$/MWh and 11 \$/MWh.

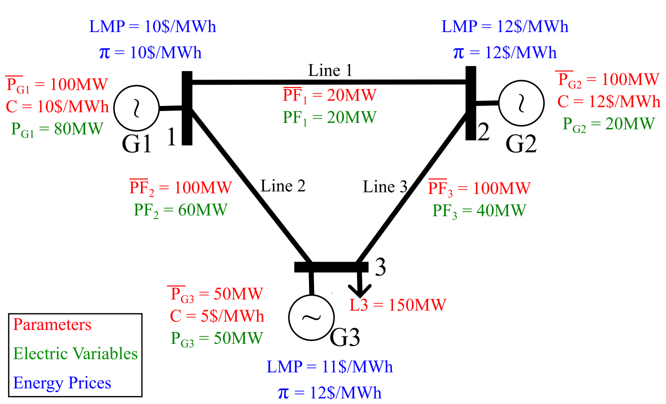

Fig. EC.2. Theoretical Example 2

Regarding the behavior of the proposed pricing mechanism in this scenario, since G1 and G2 are connected to a congested line (1-2), $w_1 \leq 1+(1-u) \implies w_1 = s_1 = s_2 = 1 \leftrightarrow u \leq 1$ (for the sake of clarity, the time and scenario subscripts are disregarded in this analysis). It should be mentioned that these variables are not forced to equal 1. Nonetheless, by doing so, CP_1 and CP_2 may be less than zero (see (28)), which decreases π_1 and π_2 to equal the node's minimum nodal price (MNP) (see (25)) and benefits the upper-level objective function. Hence, w and s will be optimized to equal 1 whenever possible. As for node 3, the energy price is equal to the system's MCP, i.e., the cost of the most expensive generator since lines 2 and 3 are not congested. The prices obtained for nodes 1, 2 and 3 using the proposed pricing method are, respectively, 10 \$/MWh, 12 \$/MWh and 12 \$/MWh.

It should be mentioned that even though $s_2=1$, the energy price of node 2 is equal to the MCP, i.e., the congestion price quota is zero ($CP_2=0$). This happens because G2 is the most expensive generator; thus, the MCP is equal to its generation cost. If $CP_2<0$, then the optimal reaction of G2 would be not to inject power, which would cause the problem to be infeasible.

Finally, consider the following power limits: 100 MW for lines 1-2 and 2-3 and 50 MW for line 1-3. The maximum power injection of each generator and optimal power flow on each line are shown in Fig. EC.3. Since G3 can no longer supply the system's demand, more expensive generators must dispatch. Additionally, note that line 1-3 is already at its limit. Therefore, any additional demand would require not only more power from G2 but also a reduction in the power injected by G1. In this kind of scenario, the LMP calculated at each node may surpass the highest generation cost [EC.4]. For this example, the calculated LMPs are 10 \$/MWh, 12 \$/MWh and 14 \$/MWh for nodes 1, 2 and 3, respectively. Increasing the energy price at a node does not inhibit power consumption in a model where the demand is inelastic. Thus, G3 is being paid more than the MCP even though the demand side is not responsive.

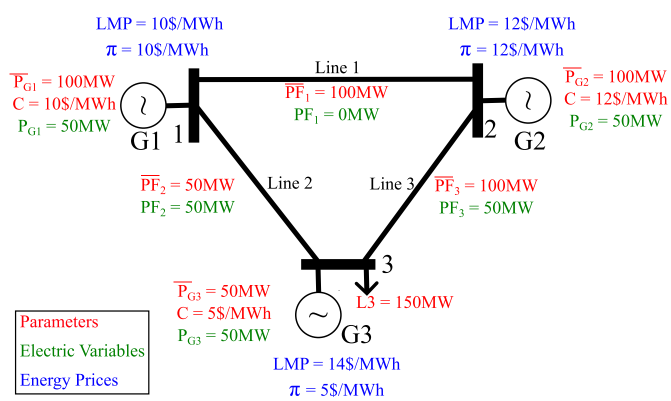

Fig. EC.3. Theoretical Example 3

The proposed pricing method considers only negative congestion price quotas (see (25) and (28)). Thus, no generator can receive more than the cost of dispatching the most expensive generator. In accordance to the previous case, $w_2 \leq 1+(1-u) \implies w_2 = s_1 = s_3 = 1 \leftrightarrow u \leq 1$. The energy prices obtained by the proposed approach are 10 \$/MWh, 12 \$/MWh and 5 \$/MWh for nodes 1, 2 and 3, respectively. Note that, although CP_1 and CP_3 are not equal to zero, G1 and G3 are not forced to operate under non-lucrative conditions.

It is worth mentioning that if $u > 1$, the model can no longer employ MNPs (rewarding method becomes strictly uniform payment) since $w_{l,t,s} < 1$, even for a scenario wherein a line reaches its capacity. Contrarily, if $u \leq 0$, the model will adopt MNPs to reward the stakeholders (rewarding method becomes strictly pay-as-bid), as paying each generator its marginal cost is the best strategy for the market operator.

IV. Test System Data

The proposed model was validated for modified versions of IEEE's 14 and 34-bus systems, employed as the transmission and distribution networks, respectively. The adopted power systems are illustrated in figs. EC.4 and EC.5. The parameters of each generator, energy storage system (ESS) and controllable load are presented in Tables EC.I, EC.II and EC.III, respectively. Data regarding the networks' physical parameters, nodal load shapes and stochastic parameters are available in [EC.5].

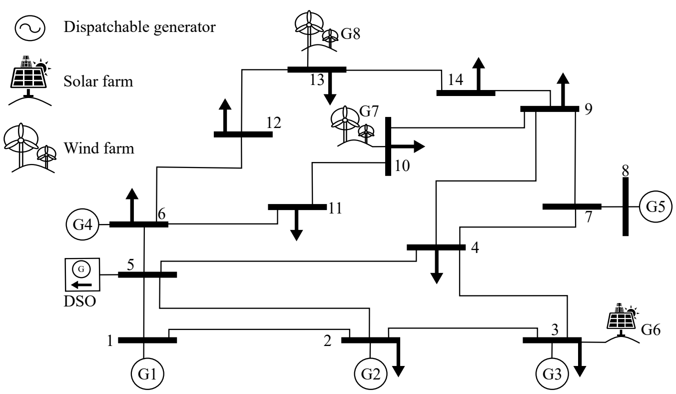

Fig. EC.4. Transmission System Illustration

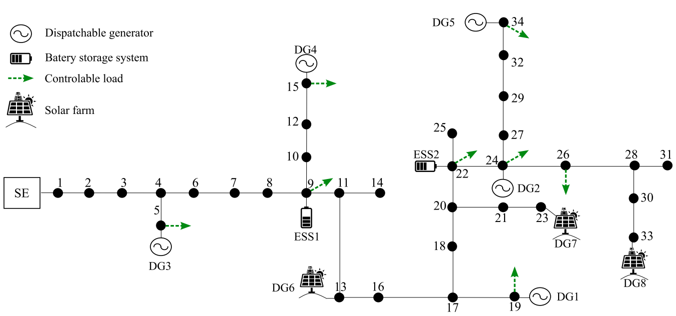

Fig. EC.5. Distribution System Illustration

References

[EC.1] J. Arroyo, "Bilevel programming applied to power system vulnerability analysis under multiple contingencies," *IET Gener. Transm. Distrib.*, vol. 4, pp. 178–190, Feb. 2010.

[EC.2] A. N. Toutounchi, S. Seyedshenava, J. Contreras, and A. Akbarimajd, "A stochastic bilevel model to manage active distribution networks with multi-microgrids," *IEEE Syst. J*, vol. 13, no. 4, pp. 4190–4199, Dec. 2019.

[EC.3] S. Bahramara, P. Sheikhahmadi, A. Mazza, G. Chicco, M. Shafie-khah, and J. P. S. Catalão, "A risk-based decision framework for the distribution company in mutual interaction with the wholesale day-ahead market and microgrids," *IEEE Trans. Industr. Inform.*, vol. 16, no. 2, pp. 764–778, Feb. 2020.

[EC.4] Y. Fu and Z. Li, "Different models and properties on lmp calculations," in *IEEE Power Engineering Society General Meeting*, Jun. 2006, pp. 1–11.

[EC.5] W. R. Faria, G. Muñoz-Delgado, J. Contreras, and B. R. Pereira Junior, "Dataset for Energy Resource Management Considering Participation in the Wholesale Day-Ahead Market," Dec. 2022. [Online]. Available: https://doi.org/10.5281/zenodo.7473796

TABLE EC.I
Generators Parameters

Generator	Cost Parameters			Power Limits		Owner
	a	b	c	$\underline{P}$ (MW)	$\overline{P}$ (MW)	
G1	0.091	29.62	0	0	30	GENCO1
G2	0.065	26.39	0	0	60	GENCO2
G3	0.010	28.31	0	0	45	GENCO3
G4	0.085	27.00	0	0	40	GENCO4
G5	0.075	27.10	0	0	20	GENCO3
G6	-	-	-	0	5	GENCO5
G7	-	-	-	0	15	GENCO5
G8	-	-	-	0	15	GENCO5
DG1	0.35	25.42	0	0	6	DSO
DG2	0.10	26.68	0	0	5	DSO
DG3	0.40	25.75	0	0	5	DSO
DG4	0.88	24.92	0	0	6	DSO
DG5	0.83	23.37	0	0	8	DSO
DG6	-	-	-	0	0.05	DSO
DG7	-	-	-	0	0.1	DSO
DG8	-	-	-	0	0.03	DSO

TABLE EC.II
Energy Storage Systems Parameters

ESS	Charging Limit (MW)	Discharging Limit (MW)	$\underline{SOC}$ (MWh)	$\overline{SOC}$ (MWh)	SOC$^{(0)}$ (MWh)
1	1	1	1	5	5
2	1	1	1	5	5

TABLE EC.III
Controllable Loads Parameters

Load	Maximum Hourly Load Increase (%)	Maximum Hourly Load Decrease (%)
L5, L15, L19	20	20
L9, L24, L34	15	15
L22, L26	10	10